

Ohmic Heating and Ionization Measurements for an Axial Discharge in Hydrogen

R. C. Cross and B. D. Blackwell

School of Physics, University of Sydney, N.S.W. 2006.

Abstract

Experimental results are presented on the heating effect and rate of ionization produced by an axial discharge (~ 10 kA) in hydrogen gas at filling pressures of 25–400 mTorr. The electron temperature remains very low (about 1.5 eV) even at ohmic heating power levels as high as 200 MW m^{-3} . The results are compared with a theoretical model which assumes that the only energy loss mechanism is ionization of neutral particles. The importance of other loss mechanisms, including convection, conduction and radiation, is also discussed.

Introduction

In this paper we examine the heating effect of a 10 kA axial discharge of current in hydrogen gas at filling pressures in the range 25–400 mTorr and in the presence of an axial magnetic field $B_z = 0.5$ T. Because of its simplicity, this method of generating a plasma is often used to study low temperature plasma phenomena or to preionize a gas prior to subsequent heating (see e.g. Malein 1965; Martone 1970; Frommelt and Jones 1975). In common with these authors we observe that the electron temperature remains very low, about 1.5 eV, even at ohmic heating power levels as high as 200 MW m^{-3} . This is in contrast to low-density ohmically heated toroidal devices, which can achieve electron temperatures exceeding 100 eV at power levels less than 0.1 MW m^{-3} . We show below that, at least during the early stages of plasma formation, the largest single contributing factor to low temperatures in a low-current high-density discharge is the ionization process. This is the same process which prevents significant electron heating in medium-speed ionizing shock waves (see e.g. Hoffert and Lien 1967).

Theory

The maximum temperature one could expect in an axial discharge of current in a radially uniform cylindrical plasma column can be estimated by ignoring thermal conduction, convection and radiation losses and assuming that the ohmic heating power is expended only in ionizing and heating an initially cold gas. We consider a constant current pulse in hydrogen with electron number density n_e , atom number density n_a , and the number density of atoms initially filling the discharge vessel being $N = n_e + n_a$. Denoting electrons, ions and atoms with subscripts e, i and a respectively, the energy equation for each species (Mitchner and Kruger 1973) can be expressed as

$$n_e d(\frac{3}{2}kT_e)/dt = \eta j_z^2 - (\frac{3}{2}kT_e + E_1) dn_e/dt - Q_{ei} - Q_{ea}, \quad (1a)$$

$$n_i d(\frac{3}{2}kT_i)/dt = Q_{ei} - Q_{ia} - \frac{3}{2}k(T_i - T_a) dn_e/dt, \quad (1b)$$

$$n_a d(\frac{3}{2}kT_a)/dt = Q_{ea} + Q_{ia}, \quad (1c)$$

where T is the temperature, η is the resistivity, j_z is the axial current density, $E_1 = 15.85$ eV is the ionization plus dissociation energy per atom and Q_{ij} is the power density (W m^{-3}) transferred from species i to species j due to elastic collisions. The electrical resistivity can be expressed as $\eta = \eta_{ea} + \eta_{ei}$ where, in SI units,

$$\eta_{ea} = \frac{4}{3}m_e \langle \sigma_{ea} \rangle \langle v_e \rangle n_a / n_e e^2 = 2.9 \times 10^{-8} (n_a/n_e) T_e^{\frac{1}{2}} \quad \Omega \text{ m} \quad (2)$$

is the contribution due to electron-atom elastic collisions, $\langle v_e \rangle = (8kT_e/\pi m_e)^{\frac{1}{2}}$ is the mean electron speed and $\langle \sigma_{ea} \rangle = 1.0 \times 10^{-19} \text{ m}^2$ is the momentum transfer cross section for elastic electron-atom collisions averaged over a Maxwellian distribution. The value of $\langle \sigma_{ea} \rangle$ decreases slowly with temperature but is essentially constant over the range $10^4 < T < 10^5$ K (Devoto 1968; Mitchner and Kruger, 1973, p. 60). The electron-ion component η_{ei} is the Spitzer (1962) resistivity

$$\eta_{ei} = 65.3 \ln(A) / T_e^{3/2}, \quad \text{where} \quad A = 1.238 \times 10^7 (T_e^3/n_e)^{\frac{1}{2}}. \quad (3)$$

Electrons transfer energy to ions at a rate (Spitzer 1962)

$$Q_{ei} = \frac{8.20 \times 10^{-32} n_e^2 \ln A}{T_e^{\frac{3}{2}}} \left(1 - \frac{T_i}{T_e}\right) \text{ W m}^{-3}, \quad (4a)$$

and to atoms, by elastic collisions, at a rate (Mitchner and Kruger, 1973, p. 51)

$$\begin{aligned} Q_{ea} &= (2m_e/m_a)^{\frac{3}{2}} k(T_e - T_a) n_e n_a \langle \sigma_{ea} \rangle \langle v_e \rangle \\ &= 1.4 \times 10^{-41} n_e n_a T_e^{\frac{1}{2}} (T_e - T_a) \text{ W m}^{-3}. \end{aligned} \quad (4b)$$

Collisions between ions and atoms result in an average energy transfer $1.5 k(T_i - T_a)$ from ions to atoms in each collision, so that the corresponding rate of transfer is

$$\begin{aligned} Q_{ia} &= 1.5 k(T_i - T_a) n_i n_a \langle \sigma_{ia} \rangle \langle v_i \rangle \\ &= 2.25 \times 10^{-39} T_i^{\frac{1}{2}} (T_i - T_a) n_i n_a \text{ W m}^{-3}, \end{aligned} \quad (4c)$$

where $\langle \sigma_{ia} \rangle = 7.5 \times 10^{-19} \text{ m}^2$ is the ion-atom cross section for momentum transfer (Cross and Lehane 1967; Devoto 1968) and $\langle v_i \rangle$ is the mean ion speed.

Bates *et al.* (1962) have calculated rates of ionization in hydrogen taking into account the large cross section for ionization from excited states as well as direct ionization from the ground state. For a plasma which is optically thick to Lyman alpha radiation, the data given by Bates *et al.* can be fitted closely by the expression

$$dn_e/dt = 2.55 \times 10^{-19} n_e n_a T_e (2 + 1.18 \times 10^5 T_e^{-1}) \exp(-1.18 \times 10^5 T_e^{-1}). \quad (5)$$

At temperatures less than 3 eV, the ionization rate is underestimated by a factor of about 100 if ionization from excited states is ignored in plasmas optically thick to L_α radiation.

The equations (1)–(5) were solved numerically assuming initial conditions $T_e = T_i = T_a = 10^3$ K and $n_e/n_a = 10^{-5}$, with values of j_z and N appropriate to the experiments described in the following section. Both j_z and N were assumed to remain constant in time except for an initial period ($t \lesssim 1 \mu\text{s}$), during which j_z was reduced to limit the voltage drop $\eta j_z d$ to the charging voltage used, that is, to ~ 10 kV (here d is the inter-electrode distance). The solutions were not sensitive to the assumed initial conditions, since T_e rises to about 10^5 K and n_e/n_a rises to about 10^{-3} in the first $0.1 \mu\text{s}$.

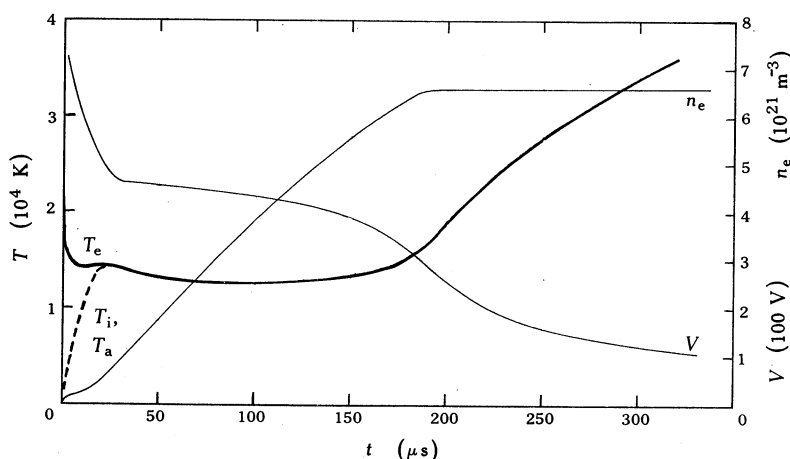


Fig. 1. Theoretical plots of the evolution in time of the electron, ion and atom temperatures T_e , T_i and T_a , the electron density n_e and the axial voltage drop V . The calculations are for a constant current $I = 10$ kA and filling pressure $p = 100$ mTorr.

The solution for $N = 6.6 \times 10^{21} \text{ m}^{-3}$, $n_e = n_i$ and $j_z = 6.49 \times 10^5 \text{ A m}^{-2}$ is shown in Fig. 1. These values correspond to an axial current $I = 10$ kA and a filling pressure of 100 mTorr in the experiment described in the following section. During the ionization phase, T_e remains approximately constant in time, since the energy gained from ohmic heating is balanced by the energy lost in ionization. If the temperature were to rise during ionization, then the rate of ionization would rise, thereby increasing the rate of energy loss. Once the gas is fully ionized, the subsequent heating rate, for $T_e = T_i = T_a$, $n_i = n_e$ and $\ln A = 5.5$, is

$$d(3n_e kT)/dt = \eta j_z^2 = 359 T^{-3/2} j_z^2. \quad (6)$$

If n_e and j_z remain constant in time, we have

$$T = (T_0^{5/2} + 2.17 \times 10^{25} n_e^{-1} j_z^2 t)^{2/5}, \quad (7)$$

where $T = T_0$ at $t = 0$.

Experimental Apparatus

The plasma source consisted of a cylindrical glass vessel of inner diameter 15.2 cm and length 265 cm, sealed at each end with a Pyrex end plate. Identical stainless steel disc electrodes of diameter 13.0 cm were mounted through the end plates, their

axial separation d being 260 cm. An axial magnetic field $B_z = 0.5$ T was maintained throughout the volume; it was constant in time and space to within 3% during plasma formation and decay. Hydrogen gas was pumped through the vessel at a constant filling pressure, the flow rate being sufficient to replace the gas between discharges. The plasma was formed by discharging a bank of ten $8.5 \mu\text{F}$, 20 kV capacitors connected, via a series ignitron, directly across the electrodes. The capacitor bank was connected as a transmission line to produce a constant current pulse of amplitude between 2 and 16 kA depending on the charging voltage. Since the impedance presented to the line was much less than its characteristic impedance ($Z = 1.06 \Omega$), the current through the plasma reversed direction every $180 \mu\text{s}$, decreasing in amplitude on each reversal (see Fig. 2).

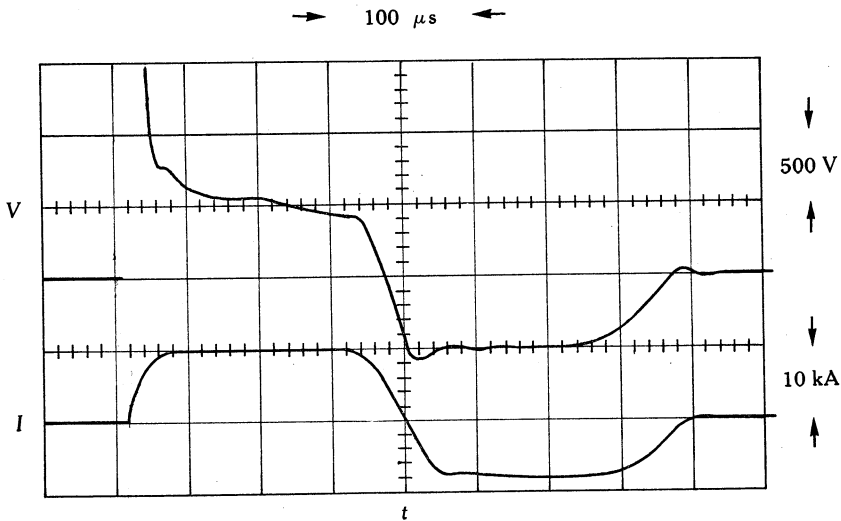


Fig. 2. Oscillograms of the time evolution of the axial voltage drop V and the input current I for a filling pressure $p = 100$ mTorr. The current was crowbarred at $350 \mu\text{s}$.

The voltage drop V between the electrodes was measured differentially to obtain an estimate of the axial electric field $E_z = V/d$. Measurements of the voltage gradient, made with the aid of tungsten tip probes inserted radially into the plasma at axial locations $z = 114$ and 206 cm, showed E_z to be constant both axially and radially to within 10%.

Radial magnetic probe measurements of the azimuthal magnetic field B_θ indicated that the plasma column remained stable during the discharge. The B_θ waveforms were similar to the current waveform at all times for $r \geq 3$ cm, but exhibited large amplitude ($\sim 70\%$ modulation) irregular fluctuations for $r < 3$ cm. These results imply that the current breaks up into moving filaments inside $r = 3$ cm, but the filaments remain evenly distributed about $r = 0$ and give a well-behaved B_θ waveform outside $r = 3$ cm. The fluctuations were not induced by the probe, since B_θ at $r \geq 3$ cm was not affected by inserting the glass probe sheath into the $r = 0$ position, and since fluctuations were not observed when the gas was changed to Argon.

The electron density was estimated from Stark broadening measurements of the H_β (486.1 nm) line. Observations were made at a radius $r = 5.5$ cm, observing axially along the discharge vessel and monitoring simultaneously a 0.2 nm band of

light centred on the H_β line and the total line intensity (a 5 nm band). The ratio of these two intensities depends on the electron density (Irons and Millar 1965) and was monitored with the simple divider circuit shown in Fig. 3. The densities obtained by this method were the same as those obtained using a more tedious complete line profile measurement.

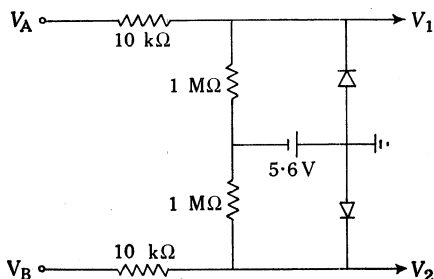


Fig. 3. Divider circuit used to monitor the time evolution of n_e . For this circuit, $\ln(V_A/V_B) = 36.5(V_1 - V_2)$. The diodes are BCY89 twin transistors with collector shorted to base.

The fractional ionization can be inferred from the observed electron densities, assuming that none of the original filling gas is lost during the discharge. This assumption was checked by measuring the total number of heavy particles (ions plus atoms) in the discharge. For this measurement, a guarded solenoid was wound on the outside of the glass vessel in order to launch a magnetoacoustic wave across a diameter of the plasma column. Impulse excitation of the wave with a short (100 ns) current pulse resulted in the excitation of a transient standing magnetoacoustic wave, which could be detected either with a magnetic probe inserted into the plasma or by measuring the voltage induced in the guarded centre section of the long solenoid. The frequency of oscillation f_0 of the standing wave was determined by the transit time of the wave across the column. For a radially uniform density distribution, f_0 is given (Blackwell and Cross 1978) by $f_0 = 0.383 V_A/a$, where a is the radius of the plasma column, $V_A = B_z/(\mu_0 \rho)^{1/2}$ is the Alfvén speed and ρ is the mass density of heavy particles coupling into the wave motion. Provided the collision frequency of an atom with ions is much larger than the wave frequency, as in this experiment, then $\rho = (n_i + n_a)m_a$.

Experimental Results

The radially averaged electron temperature during the discharge can be inferred from the voltage and current records (Fig. 2) during those periods where I remains constant in time. It can be seen from the figure that the inductive component of the voltage signal is significant only during current reversals. The resistivity of the plasma column can be equated to $\pi a^2 V/Id$, provided the induced electric field $v_r B_\theta$ is negligible compared with E_z , where v_r is the radial drift velocity of the charged species fluid. Early in the discharge, the plasma will pinch inwards at a drift speed $v_r = (E \times B)_r/B_z^2 \approx 20 \text{ ms}^{-1}$, so the $v_r B_\theta$ term remains negligible. Because of the low drift speed, it is unlikely in our experiment that an equilibrium is reached between the $j \times B$ force acting inwards and a pressure gradient acting outwards. However, an equilibrium estimate of v_r can be made on the assumption that the mass flux of ions diffusing outwards is balanced by the flux of atoms diffusing inwards. On this assumption (see equation (9) of the next section), it is estimated that $v_r B_\theta$ will not be larger than $\frac{1}{10} E_z$ at any radius.

For all the discharge conditions examined, the temperature remained constant in time to within 15% over the period $50 < t < 330 \mu\text{s}$. A comparison between observed T_{exp} and predicted T_{th} values for the time average during ionization of the radial electron temperature, assuming a plasma column radius of 7.0 cm to compute the average current density, is given in Table 1. Here T_{exp} , T_{th} and the input power density P are listed for various filling pressures at a constant discharge current of 10.0 kA (first half-cycle) and constant axial field, and also for various discharge currents at a constant filling pressure and axial field. The temperatures do not depend strongly on B_z . For $p = 100$ mTorr and $I = 10.0$ kA, the average temperature decreased by only 13% when B_z was reduced to zero. The experimental input power density P shown in the table is the mean VI product for $50 < t < 330 \mu\text{s}$ divided by the plasma volume (0.040 m^3).

Table 1. Comparison of experimental and theoretical electron temperatures in hydrogen
 T_{exp} , T_{th} and P are given as functions of p for constant I and B_z and of I for constant p and B_z

p (mTorr)	I (kA)	B_z (T)	P (MW m ⁻³)	T_{exp} (10 ⁴ K)	T_{th} (10 ⁴ K)
25	10.0	0.5	70	1.61	1.80
50	10.0	0.5	99	1.27	1.53
100	10.0	0.5	114	1.08	1.34
200	10.0	0.5	160	0.96	1.15
400	10.0	0.5	186	0.87	1.02
100	2.0	0.35	29	0.35	0.99
100	5.0	0.35	60	0.74	1.16
100	10.0	0.35	117	1.06	1.34
100	15.0	0.35	206	1.33	1.41

Fig. 4 is a plot of the electron density measurements as a function of time for $B_z = 0.5$ T, $I = 10.0$ kA (first half-cycle) and filling pressures of 25, 100 and 200 mTorr. The magnetoacoustic wave measurements confirmed that there was no loss of gas during the discharge, provided it could be assumed that a layer of neutral gas of density equal to the filling density and approximately 1 cm wide exists outside the plasma column. Evidence for a 1 cm neutral gas layer has been provided by a more detailed analysis of magnetoacoustic waves with argon as the filling gas (Blackwell and Cross 1978).

Discussion

The results obtained above indicate that ionization plays a very significant role in the early stages of plasma formation and heating, and may even be significant after n_e has attained its maximum value. Except for the $I = 2.0$ and 5.0 kA data, the observed temperatures T_{exp} given in Table 1 are close to the predicted values T_{th} , and the electron temperature for a given discharge remains constant in time, as predicted for the ionization stage of the discharge. In all cases, however, the observed electron temperature is lower than that predicted, indicating the presence of energy-loss processes. These processes dominate the behaviour of the plasma late in time, preventing the electron temperature from rising after full ionization is reached (at low filling pressures) or preventing complete ionization at high filling pressures.

The 100 mTorr results shown in Figs 2 and 4 are typical of the results obtained, and are now described in more detail. The first reliable electron density measurement (at $t = 10 \mu\text{s}$) shows that the total energy required for ionization during the first $10 \mu\text{s}$ after gas breakdown is 3.0 kJ m^{-3} . The energy input due to ohmic heating is estimated at $(4 \pm 1) \text{ kJ m}^{-3}$, the large uncertainty arising because of signal noise and the $L di/dt$ components of V in Fig. 2. Ionization therefore accounts for a major fraction of the input power early in time.

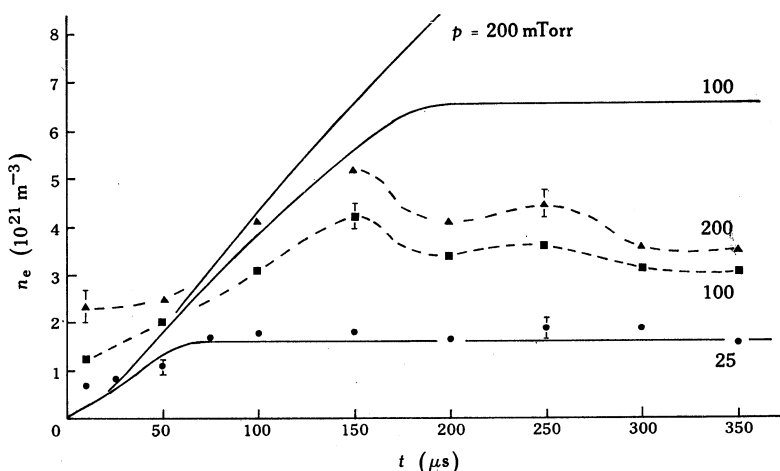


Fig. 4. Comparison of experimental (points and dashed curves) and theoretical results for the time evolution of the electron density n_e . Filling pressures (in mTorr) are indicated. The calculations assume a constant current $I = 10 \text{ kA}$ and no power loss other than ionization loss.

The initial ($t < 10 \mu\text{s}$) rapid jump in n_e at all three filling pressures was not predicted theoretically. Although the voltage waveform in Fig. 2 is qualitatively very similar to the predicted waveform (Fig. 1), the magnitude of the voltage drop, and hence power input, was much larger than predicted during the first $10 \mu\text{s}$. Both of these discrepancies (between measured and predicted n_e and V) indicate that the plasma resistivity early in time is much larger than the value given by equations (2) and (3). These equations are of doubtful validity early in time ($t < 5 \mu\text{s}$) since the kinetic energy gained during an electron mean free path is comparable with the electron thermal energy.

During the period $10 < t < 150 \mu\text{s}$, the electron density (100 mTorr dashed curve of Fig. 4) increases at a rate $2.2 \times 10^{25} \text{ m}^{-3} \text{ s}^{-1}$, corresponding to a power input for ionization of 56 MW m^{-3} . The average ohmic power input during this time is 140 MW m^{-3} . Only 5 MW m^{-3} is required to heat each new electron to the prevailing plasma temperature ($1.08 \times 10^4 \text{ K}$), so that slightly more than half the input power is being lost from the plasma. Nevertheless, the observed electron temperature remains only slightly below the value predicted ($1.34 \times 10^4 \text{ K}$) when energy loss is ignored, so that the observed voltage drop (Fig. 2) is only slightly higher than that predicted (Fig. 1). These last results are consistent with the results in Table 1, which show that the plasma temperature is not strongly sensitive to input power during ionization of the plasma. The rate of ionization, however, is a strongly varying

function of electron temperature. The rate of ionization shown in Fig. 4 at $10 < t < 150 \mu\text{s}$ is therefore considerably lower than predicted.

At $150 \mu\text{s}$, the input current begins to reverse before full ionization is reached and the electron density after current reversal remains at a level slightly lower than the peak density before reversal. Incomplete ionization is consistent with Saha equilibrium conditions at the observed temperature and indicates that, at late times, power loss mechanisms balance the ohmic power input. At lower pressures (e.g. the 25 mTorr results in Fig. 4) the gas appears to be fully ionized by $150 \mu\text{s}$, but the electron temperature does not rise in the reverse current cycle, again indicating a balance between power loss mechanisms and power input. In all observed cases, the plasma temperature during the reverse current cycle remained within 15% of the temperature during the first cycle of current.

The theoretical results described above show that the continued presence of neutral gas within the body of a plasma will prevent any significant temperature rise. Fig. 1 reveals that a temperature rise occurs only when the percentage ionization exceeds about 95%. The 25 mTorr result is therefore somewhat surprising, since the temperature remains constant even after the gas appears to be fully ionized. This result strongly suggests that the 25 mTorr plasma is never fully ionized, but that a small percentage of neutral gas remains to keep the temperature constant. An important energy loss mechanism may therefore involve a continuous cycle in which charged particles diffuse out of the plasma, recombine near the wall and diffuse back into the plasma as neutral atoms. In order to produce a net energy loss from the plasma, additional mechanisms are needed to transfer thermal and ionization energy from the charged particles to the wall region.

A detailed estimate of the power loss mechanisms has not been attempted because of the complexity of the processes thought to be involved. Electron thermal conduction parallel to B_z represents only a minor loss mechanism because of the small axial temperature gradient. Electron and ion thermal conduction perpendicular to B_z is also negligible theoretically and this is supported by a simple experimental observation. The perpendicular thermal conductivity of ions and electrons depends strongly on B_z , but the plasma temperature was found to be almost independent of B_z . According to the calculations of Bates and Kingston (1963, 1964) the power radiated from the plasma amounts to less than 10% of the input power for all conditions studied. At $T_e = 10^4 \text{ K}$, the mean free path of L_α photons is 0.1 mm at $n_a = 1.7 \times 10^{21} \text{ m}^{-3}$ (the 25 mTorr filling density). Some of these photons will diffuse out of the plasma, but a more important loss mechanism may be the multistep process in which excited-state atoms transfer the excitation energy (10.2 eV) to electrons via superelastic collisions, and the electrons transfer this energy to atoms by elastic electron-atom collisions and by electron-ion then ion-atom collisions. Because of the high thermal conductivity of neutral hydrogen (Yos 1963; Devoto 1968) energy transferred to atoms is conducted rapidly to the walls. Calculations based on Yos's data (which include the high conductivity peak due to dissociation of H_2 molecules) indicate that the total ohmic power generated in the plasma can conceivably be conducted via neutral gas to the wall. For example, a temperature drop from 6×10^3 to 300 K over a distance of 5 mm will produce a power flux $3.5 \times 10^6 \text{ W m}^{-2}$. This flux corresponds to the ohmic power input for the $I = 10 \text{ kA}$, $p = 100 \text{ mTorr}$ conditions.

An estimate of the diffusion loss can be made assuming an equilibrium situation where the plasma as a whole is at rest and the radial current density is zero. In this case, the radial diffusion velocities v_{ri} and v_{re} of ions and electrons are equal, and the radial diffusion velocity v_{ra} of atoms is given by $n_a v_{ra} = -n_i v_{ri}$. The net power flux W convected in the radial direction is then

$$W = n_i v_{ri}(1.5 kT + E_i) \quad \text{W m}^{-2},$$

assuming all species are at the same temperature T . An expression for v_{ri} can be obtained from the atom momentum equation

$$n_a m_a \partial v_a / \partial t = -\nabla p_a + n_i m_i v_{ia}(v_i - v_a), \quad (8)$$

where $p_a = n_a kT_a$. In equilibrium, the radial component of equation (8) yields

$$v_{ri} = \frac{n_a}{n_i m_i v_{ia}(n_i + n_a)} \frac{\partial p_a}{\partial r}. \quad (9)$$

If we assume further that the total pressure gradient in the plasma is zero and the plasma is in Saha equilibrium, W can be expressed in terms of a reactive contribution to the thermal conductivity (Devoto 1968). Calculations based on this model indicate that convection losses may account for 20%–30% of the total power loss. However, atoms diffusing from the wall take a relatively long time to ionize, and will build up on axis to a value exceeding the Saha equilibrium value. Small departures from Saha equilibrium can be expected to have a significant effect on the reactive contribution to thermal conductivity, since n_a and hence $\partial p_a / \partial r$ in equation (9) are strongly varying functions of temperature.

Acknowledgments

Support for this work has been provided by the Australian Research Grants Committee, the Australian Institute of Nuclear Science and Engineering, the University of Sydney Research Grants Committee and the Science Foundation for Physics within the University of Sydney.

References

- Bates, D., and Kingston, A. (1963). *Planet. Space Sci.* **11**, 1.
- Bates, D., and Kingston, A. (1964). *Proc. R. Soc. London* **279**, 10.
- Bates, D., Kingston, A., and McWhirter, R. (1962). *Proc. R. Soc. London A* **270**, 155.
- Blackwell, B., and Cross, R. (1978). Remote plasma probing with magnetoacoustic waves. *J. Plasma Phys.* (in press).
- Cross, R., and Lehan, J. (1967). *Aust. J. Phys.* **21**, 129.
- Devoto, R. (1968). *J. Plasma Phys.* **2**, 617.
- Frommelt, J., and Jones, I. (1975). *J. Plasma Phys.* **14**, 373.
- Hoffert, M., and Lien, H. (1967). *Phys. Fluids* **10**, 1769.
- Irons, F., and Millar, D. (1965). *Aust. J. Phys.* **18**, 23.
- Malein, A. (1965). *Nucl. Fusion* **5**, 352.
- Martone, M. (1970). *Nuovo Cimento B* **68**, 91.
- Mitchner, M., and Kruger, C. (1973). 'Partially Ionized Gases' (Wiley: New York).
- Spitzer, L. (1962). 'Physics of Fully Ionised Gases', 2nd edn (Interscience: New York).
- Yos, J. (1963). AVCO Tech. Memo. No. RAD-TM-63-7.

